

Supplementary Information:

Gold-linked strings of donor-acceptor dyads: On-surface formation and mutual orientation

Sujoy Karan,^{*,†,¶} Yan Geng,^{‡,§} Silvio Decurtins,[‡] Shi-Xia Liu,[‡] and Jascha Repp[†]

*†Institute of Experimental and Applied Physics, University of Regensburg, 93053
Regensburg, Germany*

‡Department of Chemistry and Biochemistry, University of Bern, 3012 Bern, Switzerland

*¶Present address: Max Planck Institute for Solid State Research, Heisenbergstraße 1,
70569 Stuttgart, Germany, E-mail: s.karan@fkf.mpg.de*

*§Present address: College of Chemistry, Chemical Engineering and Material Science,
Shandong Normal University, Jinan 250014, P. R. China*

E-mail: sujoy.karan@physik.uni-regensburg.de

Synthesis of dibromo-TTF-BTD

4,8-Dibromo[1,3]dithiolo[4,5-*f*]-2,1,3-benzothiadiazol-6-one was prepared following procedures reported in the literature.^{1,2} Commercially available reagents were used without additional purification. ¹H spectrum was recorded on a BrukerAvance 300 spectrometer operating at 300 MHz. Chemical shifts are reported in parts per million (ppm) and are referenced to the residual solvent peak (DMSO-*d*₆ 2.50 ppm). HRMS data was obtained with ESI (electrospray ionization) mode. Melting point was measured with Büchi B-540 microscope apparatus. Infrared spectrum was recorded on a Perkin-Elmer Spectrum One FT-IR spectrometer. Elemental analysis was performed on a Carlo Erba EA 1110 CHNS apparatus.

Triethylphosphite (4 mL) was added to a solution of 4,8-dibromo[1,3]dithiolo[4,5-*f*]-2,1,3-benzothiadiazol-6-one (58 mg, 0.15 mmol) and vinylene trithiocarbonate (54 mg, 0.4 mmol) in toluene (2 mL) under Ar. The mixture was refluxed for 3 h before cooling to room temperature. The resultant precipitate was filtered off and washed with MeOH. The crude product was purified by column chromatography on silica gel using a mixture of hexane/dichloromethane (1/1) as eluent to afford dibromo-TTF-BTD as purple solid. Yield: 25 mg (35%); m.p. >350°C; IR (KBr): $\tilde{\nu}$ = 3437, 3068, 1633, 1546, 1515, 1470, 1456, 1400, 1302, 1261, 1196, 1029, 995, 871, 834, 799, 778, 735, 678, 670, 643, 573 cm⁻¹; ¹H NMR: δ 6.70 (singlet) ppm; ¹³C NMR is unavailable due to poor solubility; HRMS (ESI): *m/z* calcd for C₁₀H₂Br₂N₂S₅: 467.7188; found: 467.7183; Elemental analysis calcd (%) for C₁₀H₂Br₂N₂S₅: C 25.54, H 0.43, N 5.96; found: C 25.88, H 0.46, N 5.72.

Autocorrelation of simulated chains

To better understand the autocorrelation analysis of the experimentally observed alignment of molecular units in the polymeric chain, such a chain formation was mimicked in a simple Mont-Carlo simulation. To this end, a sequence of two elements $-1, +1$ was generated, representing the two possible orientations of each unit. The orientation of every new unit was chosen based on random numbers and certain alignment probabilities which were entered as parameters (discussed below). The resulting sequence was analyzed in terms of autocorrelation in the very same way as the experimentally observed alignment of monomers was analyzed.

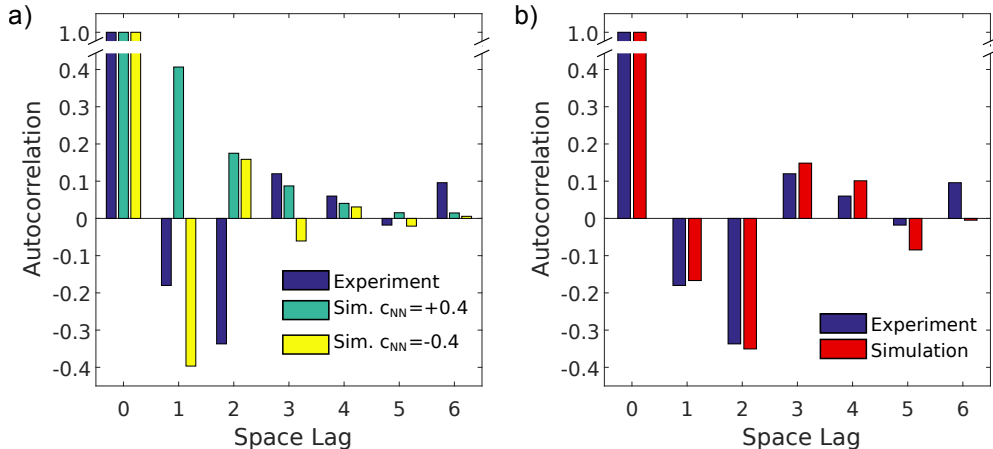


Figure S1: Comparison of the autocorrelation analysis of experimental polymer chains to Monte-Carlo simulations. (a) If only a nearest-neighbor correlation is considered in the simulation, the experimental behavior could not be reproduced. (b) The simulation taking a nearest-neighbor and a next-nearest-neighbor correlation into account leads to a good agreement with the experiment.

Figure S1 shows the comparison of the autocorrelation derived from the experiment and the simulations. In a first set of simulations, only a nearest-neighbor correlation c_{NN} was considered. Hence, the probability for the alignment of every new unit depended on the previous unit only. Irrespective of the choice of parameter c_{NN} the experimental behavior could not be reproduced even qualitatively, as can be seen in Fig. S1a. This discrepancy can be grasped best for the correlation of next-nearest-neighbors: if only a nearest-neighbor

correlation is taken into account, the next-nearest-neighbor correlation is simply given by c_{NN}^2 , which is always positive, irrespective of the sign of c_{NN} . However, the experimental next-nearest-neighbor correlation is negative.

In contrast, if in the simulations the alignment of every new element depends (with certain probability) on the alignment of the *two* preceding elements, the experimental autocorrelation trace can be reproduced very well, see Fig. S1b. In the latter simulations the nearest-neighbor correlation was set to $c_{\text{NN}} = -0.24$, while an additional, explicit next-nearest-neighbor correlation of -0.38 was assumed.

References

- (1) F. Pop, A. Amacher, N. Avarvari, J. Ding, L. M. L. Daku, A. Hauser, M. Koch, J. Hauser, S.-X. Liu and S. Decurtins, *Chem. Eur. J.*, 2013, **19**, 2504.
- (2) H.-P. Jia, J. Ding, Y.-F. Ran, S.-X. Liu, C. Blum, I. Petkova, A. Hauser and S. Decurtins, *Chem. Asian J.*, 2011, **6**, 3312.